ADP-09-10/T688

Isolating the Roper Resonance in Lattice QCD

M.S. Mahbub[a,b], Alan Ó Cais[a,c], Waseem Kamleh[a], Ben G. Lasscock[a], Derek B. Leinweber[a], Anthony G. Williams[a]

[a] *Special Research Centre for the Subatomic Structure of Matter, Adelaide, South Australia 5005, Australia, and Department of Physics, University of Adelaide, South Australia 5005, Australia.*
[b] *Department of Physics, Rajshahi University, Rajshahi 6205, Bangladesh.*
[c] *Cyprus Institute, Guy Ourisson Builiding, Athalassa Campus, PO Box 27456, 1645 Nicosia, Cyprus.*

Abstract

We present results for the first positive parity excited state of the nucleon, namely, the Roper resonance ($N^{\frac{1}{2}^+}$=1440 MeV) from a variational analysis technique. The analysis is performed for pion masses as low as 224 MeV in quenched QCD with the FLIC fermion action. A wide variety of smeared-smeared correlation functions are used to construct correlation matrices. This is done in order to find a suitable basis of operators for the variational analysis such that eigenstates of the QCD Hamiltonian may be isolated. A lower lying Roper state is observed that approaches the physical Roper state. To the best of our knowledge, the first time this state has been identified at light quark masses using a variational approach.

Key words: Roper resonance, Roper state, Positive parity, Excited state
PACS: 11.15.Ha, 12.38.Gc, 12.38.-t, 13.75.Gx

One of the long-standing puzzles in hadron spectroscopy has been the low mass of the first positive parity, $J^P = \frac{1}{2}^+$, excitation of the nucleon, known as the Roper resonance $N^*(1440$ MeV). In constituent or valence quark models with harmonic oscillator potentials, the lowest-lying odd parity state naturally occurs below the $N = \frac{1}{2}^+$ state (with principal quantum number $N = 2$) [1, 2] whereas, in nature the Roper resonance is almost 100 MeV below the $N = \frac{1}{2}^-(1535$ MeV) state. Similar difficulties in the level orderings appear for the $J^P = \frac{3}{2}^+\Delta^*(1600)$ and $\frac{1}{2}^+\Sigma^*(1690)$ resonances, which have led to the speculation that the Roper resonance may be more appropriately viewed as a hybrid baryon state with explicitly excited gluon field configurations [3, 4], or as a breathing mode of the ground state [5] or states which can be described in terms of meson-baryon dynamics alone [6].

The first detailed analysis of the positive parity excitation of the nucleon was performed in Ref. [7] using Wilson fermions and an operator product expansion spectral ansatz. Since then several attempts have been made to address these issues in the lattice framework [8, 9, 10, 11, 12, 13, 14, 15, 16, 17], but in many cases no potential identification of the Roper state has been made [8, 9, 10, 11, 12]. Recently however, in the analysis of [13, 14, 18], a low-lying Roper state has been identified using Bayesian techniques.

Here, we use a 'variational method' [19, 20, 21], which is based on a correlation matrix analysis and has been used quite extensively in Refs. [11, 16, 21, 22, 23, 24, 25, 26, 27, 28, 29, 30, 31, 32, 33, 34, 35, 36, 37]. Though the ground state mass of the nucleon has been described successfully, an unambiguous determination of the Roper state with this method has not been achieved in the past, though significant amounts of research have been carried out in Ref. [23], by the CSSM Lattice Collaboration [11, 16, 25], the BGR [26, 27, 28, 29, 33] Collaboration and in Refs. [36, 37]. In this Letter, we present evidence of a low-lying Roper state for the first time using a variational analysis. The observed state displays chiral curvature and approaches the physical mass of the Roper state. The standard nucleon interpolating field χ_1 is considered in this analysis. Various sweeps of Gaussian smearing [38] are used to construct a smeared-smeared correlation function basis from which we obtain the correlation matrices.
The two point correlation function matrix for $\vec{p} = 0$ can

be written as

$$G_{ij}(t) = (\sum_{\vec{x}} \mathrm{Tr}_{\mathrm{sp}}\{\Gamma_{\pm}\langle\Omega|\chi_i(x)\overline{\chi}_j(0)|\Omega\rangle\}) \quad (1)$$

$$= \sum_{\alpha} \lambda_i^{\alpha}\overline{\lambda}_j^{\alpha} e^{-m_{\alpha}t}, \quad (2)$$

where, Dirac indices are implicit. Here, λ_i and $\overline{\lambda}_j$ are the couplings of interpolators χ_i and $\overline{\chi}_j$ at the sink and source, respectively. α enumerates the energy eigenstates with mass m_α.

Since the only t dependence comes from the exponential term, one can seek a linear superposition of interpolators, $\overline{\chi}_j u_j^{\alpha}$, such that (more detail can be found in Refs. [11, 16]),

$$G_{ij}(t+\triangle t)\, u_j^{\alpha} = e^{-m_{\alpha}\triangle t}\, G_{ij}(t)\, u_j^{\alpha}, \quad (3)$$

for sufficiently large t and $t+\triangle t$, see Refs. [22] and [16]. Multiplying the above equation by $[G_{ij}(t)]^{-1}$ from the left leads to an eigenvalue equation,

$$[(G(t))^{-1}G(t+\triangle t)]_{ij}\, u_j^{\alpha} = c^{\alpha}\, u_i^{\alpha}, \quad (4)$$

where $c^{\alpha} = e^{-m_{\alpha}\triangle t}$ is the eigenvalue. Similar to Eq.(4), one can also solve the left eigenvalue equation to recover the v^{α} eigenvector,

$$v_i^{\alpha}\,[G(t+\triangle t)(G(t))^{-1}]_{ij} = c^{\alpha} v_j^{\alpha}. \quad (5)$$

The vectors u_j^{α} and v_i^{α} diagonalize the correlation matrix at time t and $t+\triangle t$ making the projected correlation matrix,

$$v_i^{\alpha} G_{ij}(t) u_j^{\beta} \propto \delta^{\alpha\beta}. \quad (6)$$

The parity projected, eigenstate projected correlator,

$$v_i^{\alpha} G_{ij}^{\pm}(t) u_j^{\alpha} \equiv G_{\pm}^{\alpha}, \quad (7)$$

is then analyzed using standard techniques to obtain masses of different states.

Our analysis is exploratory, seeking to develop techniques to access the Roper state in lattice gauge theory. Our lattice ensemble consists of 200 quenched configurations with a lattice volume of $16^3 \times 32$. Gauge field configurations are generated by using the DBW2 gauge action [39, 40] and an $O(a)$-improved FLIC fermion action [41] is used to generate quark propagators. This action has excellent scaling properties and provides near continuum results at finite lattice spacing [42]. The lattice spacing is $a = 0.1273$ fm, as determined by the static quark potential, with the scale set using the Sommer scale, $r_0 = 0.49$ fm [43]. In the irrelevant operators of the fermion action we apply four sweeps of stout-link smearing to the gauge links to reduce the coupling with the high frequency modes of the theory [44] providing $O(a)$ improvement [42]. We use the same method as in Ref. [16, 45] to determine fixed boundary effects, and the effects are significant only after time slice 25 in the present analysis. Various sweeps (1, 3, 7, 12, 16, 26, 35, 48 sweeps corresponding to rms radii, in lattice units, of 0.6897, 1.0459, 1.5831, 2.0639, 2.3792, 3.0284, 3.5237, 4.1868) of gauge invariant Gaussian smearing [38] are applied symmetrically at the source (at $t = 4$) and at the sink. This is to ensure a variety of overlaps of the interpolators with the lower-lying states. The analysis is performed on ten different quark masses corresponding to pion masses $m_\pi = \{0.797, 0.729, 0.641, 0.541, 0.430, 0.380, 0.327, 0.295, 0.249, 0.224\}$ GeV. Error analysis is performed using a second-order single elimination jackknife method, where the χ^2/dof is obtained via a covariance matrix analysis method. Our fitting method is discussed extensively in Ref. [16].

The nucleon interpolator we consider is the local scalar-diquark interpolator having a non-relativistic reduction [7, 46],

$$\chi_1(x) = \epsilon^{abc}(u^{Ta}(x)\, C\gamma_5\, d^b(x))\, u^c(x). \quad (8)$$

We consider several 4×4 matrices. Each matrix is constructed with different sets of correlation functions, each set element corresponding to a different numbers of sweeps of gauge invariant Gaussian smearing at the source and sink of the $\chi_1\overline{\chi}_1$ correlators. This provides a large basis of operators with varieties of overlap among energy states. We consider seven combinations {1=(1,7,16,35), 2=(3,7,16,35), 3=(1,12,26,48), 4=(3,12,26,35), 5=(3,12,26,48), 6=(12,16,26,35), 7=(7,16,35,48)} of 4×4 matrices. In Ref. [16] it was shown that one cannot isolate a low-lying excited eigenstate using a single fixed-size source smearing. The superposition of states manifested itself as a smearing dependence of the effective mass. In this Letter we exploit this sensitivity to isolate the energy eigenstates.

In Fig.1, we show the mass from the projected correlation functions and from the eigenvalues (as shown in Ref. [16]) for the fourth combination (3,12,26,35) of 4×4 matrices. We note that similar results in mass from the projected correlation functions and the eigenvalues are observed in this analysis as in Ref. [16]. Though the mass of the first excited state from projected correlation functions show little change with variational parameters, see Fig.1, the second and third excited states start a little below which indicates t and $t+\triangle t$ are not sufficiently large. With larger Euclidean times fewer states

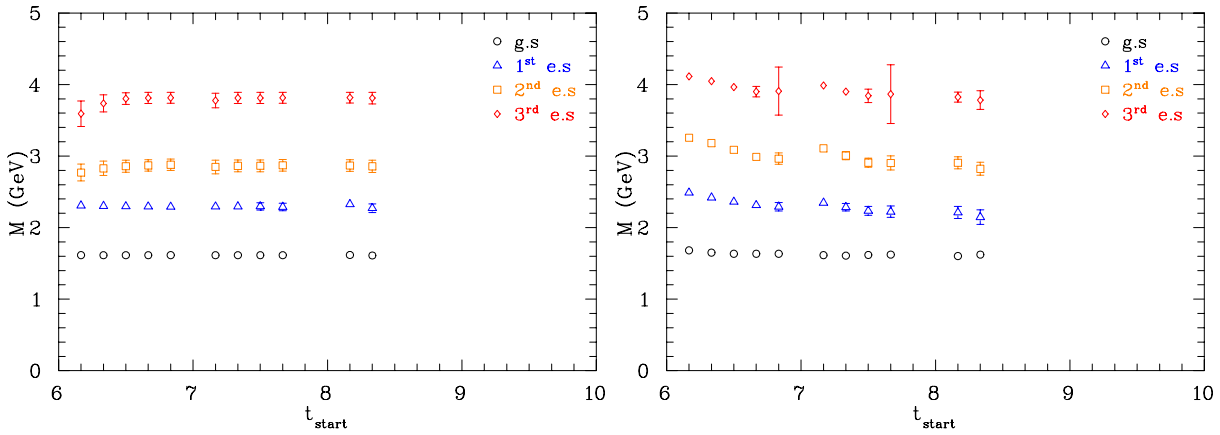

Figure 1: (Color online). Masses of the nucleon, $N^{\frac{1}{2}^+}$ - states, from projected correlation functions as shown in Eq.(7) (left figure) and from eigenvalues (right figure), for the pion mass of 797 MeV, and for the 4$^{\text{th}}$ combination (3,12,26,35) of 4×4 matrices. Each set of ground and excited states masses correspond to the diagonalization of the correlation matrix for each set of variational parameters $t \equiv t_{\text{start}}$ (shown in major tick marks) and $\triangle t$ (shown in minor tick marks). In the legend "g.s" stands for the ground state, whereas, "e.s" is for excited state. Larger values of t_{start} and $\triangle t$ did not provide a stable eigenvalue analysis.

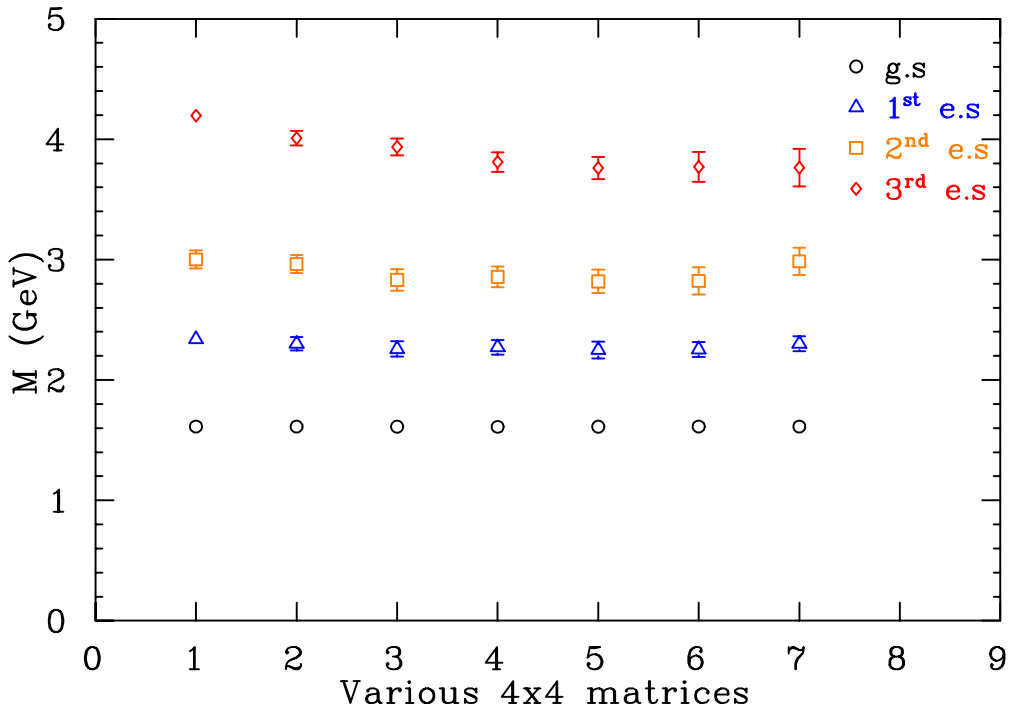

Figure 2: (Color online). Masses of the nucleon, $N^{\frac{1}{2}^+}$ - states, from projected correlation functions as shown in Eq.(7) for the pion mass of 797 MeV. Numbers in the horizontal scale correspond to each combination of smeared 4×4 correlation matrices. For instance, 1 and 2 correspond to the combinations of (1,7,16,35) and (3,7,16,35) respectively and so on, as discussed in the text following Eq.(8). Masses are extracted according to the selection criteria described in Ref. [16].

will contribute significantly to the correlators. The robust aspect of fitting projected correlators is manifest in Fig.1, and reflects the stability of the eigenvectors against changes in t and $t + \triangle t$. In contrast, the mass from the eigenvalue analysis shows significant dependence on the variational parameters. The same method as described in Ref. [16] is applied in this Letter to extract the mass from the projected correlation functions.

In Fig.2, masses extracted from all the combinations of 4×4 matrices (from 1^{st} to 7^{th}) are shown for the pion mass of 797 MeV. Some dependence of the excited states on smearing count is also observed here as in Ref. [16] for a few of the interpolator basis smearing sets. However the ground and first excited states are robust against changes in the interpolator basis, providing evidence that an energy eigenstate has been isolated. It should be noted that the highest excited state (the third excited state) is influenced more by the level of smearing than the lower excited states. This is to be expected as this state must accommodate all remaining spectral strength.

The 1^{st} combination in Fig.2 provides heavier excited states as this basis begins with a low number of smearing sweeps (a sweep count of 1) and also contains another low smearing set of 7 sweeps. The second and third excited states, and more importantly, the first excited state sits a bit high in comparison with the other bases. Hence, extracting masses with this basis is not as reliable as other sets. The 2^{nd} combination also contains elements with a small smearing sweep count (3 and 7), hence this basis also provides heavier excited states and shows some systematic drift in the second excited state. However, this basis has reduced contamination from the excited states when compared with the first basis. The 3^{rd} combination also starts at the low smearing count, so the mass from this basis for the third excited state is a little high.

We can observe at this point that including basis elements with a low smearing count will increase the masses of excited states (for instance, consecutive low numbers of smearing sweeps 1,7 and 3,7, respectively). This is because the correlation functions with these low sweep counts have a large overlap with several heavier excited states in their sub-leading exponential. We also observe that the inclusion of basis elements with a high level of smearing (for instance, a sweep count of 48) results in larger statistical errors in the analysis.

The 6^{th} combination starts from a moderate smearing sweep count (12) and also contains elements with consecutive smearing sweep counts which provides less diversity in the basis. Similarly, the 7^{th} combination contains consecutive large smearing sweep counts of 35 and 48 and operators for these levels of smearing are very similar challenging the isolation of single energy eigenstates.

The 4^{th} and 5^{th} combinations are well spread over the given range of smearing sweeps and start from a sweep count of 3. They don't include successive lower smearing sweep counts. The 5^{th} combination contains the basis element with a sweep count of 48 but has only slightly larger statistical errors than the 4^{th} basis choice. Both these bases provide diversity. It is observed that both combinations provide consistent results for the states. Nonetheless, it should be noted that the 3^{rd} to 6^{th} combinations all provide very consistent results for the lower three (ground, first and second) energy states, shown in Fig.2. While the 2^{nd} and the 3^{rd} excited states display some evidence of eigenstate mixing, the ground and the 1^{st} excited states are robust in this analysis as they agree within one standard deviation for all the combinations of 4×4 matrices. Hence, an analysis is performed to calculate the systematic errors associated with the choice of basis over the preferred four combinations (from 3^{rd} to 6^{th}) with $\sigma_b = \sqrt{\frac{1}{N_b - 1} \sum_{i=1}^{N_b} (M_i - \bar{M})^2}$, where, N_b is the number of bases, in this case is equal to 4. It should be noted that for the ground and first excited states the systematic errors associated with choice of basis are very small in comparison with their statistical errors (see Table 1).

In Fig.3, the masses from projected correlation functions are shown for all pion masses averaged over four combinations of correlation matrices (from 3^{rd} to 6^{th}). Masses are averaged over these four bases and errors (average statistical errors over these four bases and systematic errors associated with basis choices) are combined in quadrature, $\sigma = \sqrt{\bar{\sigma}_s^2 + \sigma_b^2}$. Eigenstate mixing may be affecting the results for the second and the third excited states. The ground and the 1^{st} excited states systematically approach the physical mass of the Nucleon and Roper state. This is the first time evidence of a low-lying Roper state has appeared from variational analysis near the chiral regime.

In Fig.4, the ground and the first excited states of Fig.3 are shown in larger scale for clarity. The non-interacting two particle P-wave $N + \pi$ is shown by the dashed line. It is interesting to note that the observed lattice Roper state sits lower than the P-wave $N + \pi$, indicative of attractive πN interactions producing a resonance at physical quark masses. The very consistent Euclidean-time fit window for all the bases and for all the quark masses, noticeably the lower time of the fit as shown in Table 2, assist to identify the robust nature of the extracted Roper state which comes at the same

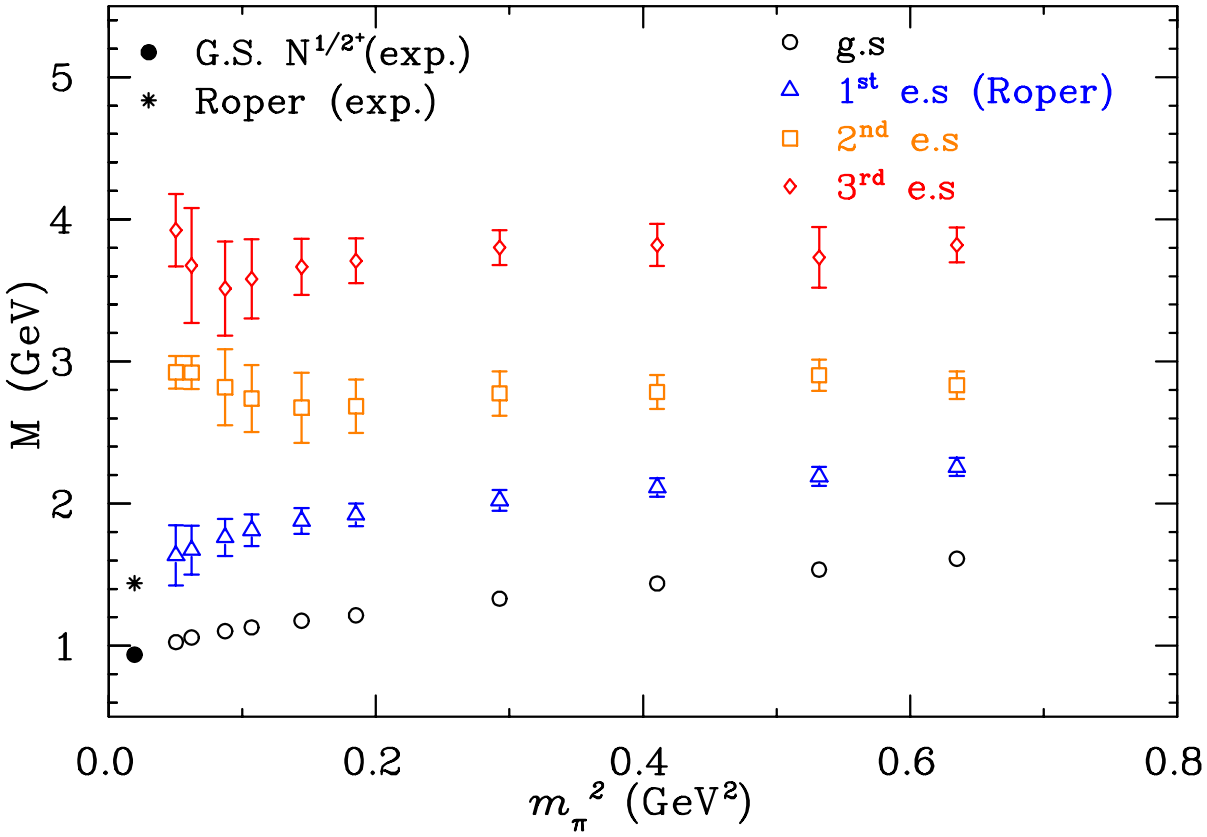

Figure 3: (Color online). Mass of the nucleon, $N^{\frac{1}{2}^+}$ - states, for the ground and the excited states. The errors shown in the figure are a combination of average statistical errors and systematic errors due to basis choices over four bases (from 3rd to 6th of Fig.2). Errors are combined in quadrature. The black filled symbols are the experimental values of the ground and the Roper states of the nucleon [47]. The rightmost point corresponds to the pion mass of 797 MeV, then for 739, 641, 541, 430, 380, 327, 295, 249 and 224 MeV (leftmost point).

Table 1: Mass of the nucleon, $N^{\frac{1}{2}^+}$ - states, are averaged over the four bases (from 3rd to 6th) and the errors for the nucleon shown here are a combination of average statistical errors and systematic errors for choice of basis over the four bases. The 2nd and 3rd states may be superposition of energy eigenstates as discussed in the text.

aM_π	$aM^{N^{\frac{1}{2}^+}}_{g.s}$	$aM^{N^{\frac{1}{2}^+}}_{1^{st}\ e.s}$(Roper)	$aM^{N^{\frac{1}{2}^+}}_{2^{nd}\ e.s}$	$aM^{N^{\frac{1}{2}^+}}_{3^{rd}\ e.s}$
0.5141(19)	1.0399(65)	1.457(41)	1.827(62)	2.464(78)
0.4705(20)	0.9905(71)	1.413(43)	1.872(71)	2.40(13)
0.4134(22)	0.9280(79)	1.364(42)	1.797(77)	2.464(95)
0.3490(24)	0.8589(90)	1.304(46)	1.79(10)	2.452(78)
0.2776(24)	0.783(11)	1.239(51)	1.73(12)	2.39(10)
0.2452(24)	0.758(13)	1.212(58)	1.72(15)	2.36(12)
0.2110(27)	0.728(13)	1.169(71)	1.76(15)	2.30(17)
0.1905(31)	0.711(12)	1.137(83)	1.81(17)	2.26(21)
0.1607(35)	0.682(13)	1.07(11)	1.885(74)	2.37(26)
0.1448(44)	0.661(15)	1.05(13)	1.885(73)	2.53(16)

Table 2: Mass of the Roper state, $N^{\frac{1}{2}^+}$, for four bases {(1,12,26,48), (3,12,26,35), (3,12,26,48) and (12,16,26,35)} of 4×4 matrices. t_1 and t_2 represent the lower and upper times respectively of fit windows in the projected effective mass. Inclusion of $t_1 = 6$ produces $\chi^2/\text{dof} \gg 1$.

3rd basis (1,12,26,48)				4th basis (3,12,26,35)				5th basis (3,12,26,48)				6th basis (12,16,26,35)			
t_1	t_2	aM (Roper)	$\frac{\chi^2}{\text{dof}}$	t_1	t_2	aM (Roper)	$\frac{\chi^2}{\text{dof}}$	t_1	t_2	aM (Roper)	$\frac{\chi^2}{\text{dof}}$	t_1	t_2	aM (Roper)	$\frac{\chi^2}{\text{dof}}$
7	12	1.456(41)	0.58	7	12	1.465(39)	0.63	7	12	1.451(44)	0.51	7	12	1.454(40)	0.57
7	12	1.411(43)	0.55	7	12	1.419(41)	0.62	7	12	1.405(46)	0.48	7	12	1.417(39)	0.60
7	12	1.368(39)	0.54	7	12	1.361(45)	0.60	7	12	1.364(40)	0.53	7	11	1.363(42)	0.68
7	12	1.307(44)	0.57	7	11	1.298(51)	0.60	7	12	1.305(45)	0.57	7	10	1.308(46)	0.54
7	11	1.235(50)	0.43	7	11	1.245(51)	0.57	7	11	1.233(51)	0.37	7	11	1.244(52)	0.38
7	11	1.210(60)	0.42	7	11	1.211(55)	0.58	7	11	1.206(57)	0.38	7	11	1.220(60)	0.49
7	10	1.163(69)	0.60	7	11	1.165(67)	0.56	7	10	1.164(71)	0.53	7	10	1.184(75)	0.56
7	10	1.129(82)	0.61	7	10	1.127(81)	0.84	7	10	1.136(82)	0.58	7	10	1.155(85)	0.54
7	10	1.07(10)	0.56	7	10	1.06(10)	0.95	7	10	1.07(11)	0.68	7	10	1.11(11)	0.63
7	9	1.04(13)	0.85	7	10	1.01(12)	0.97	7	9	1.05(13)	0.79	7	9	1.10(13)	0.70

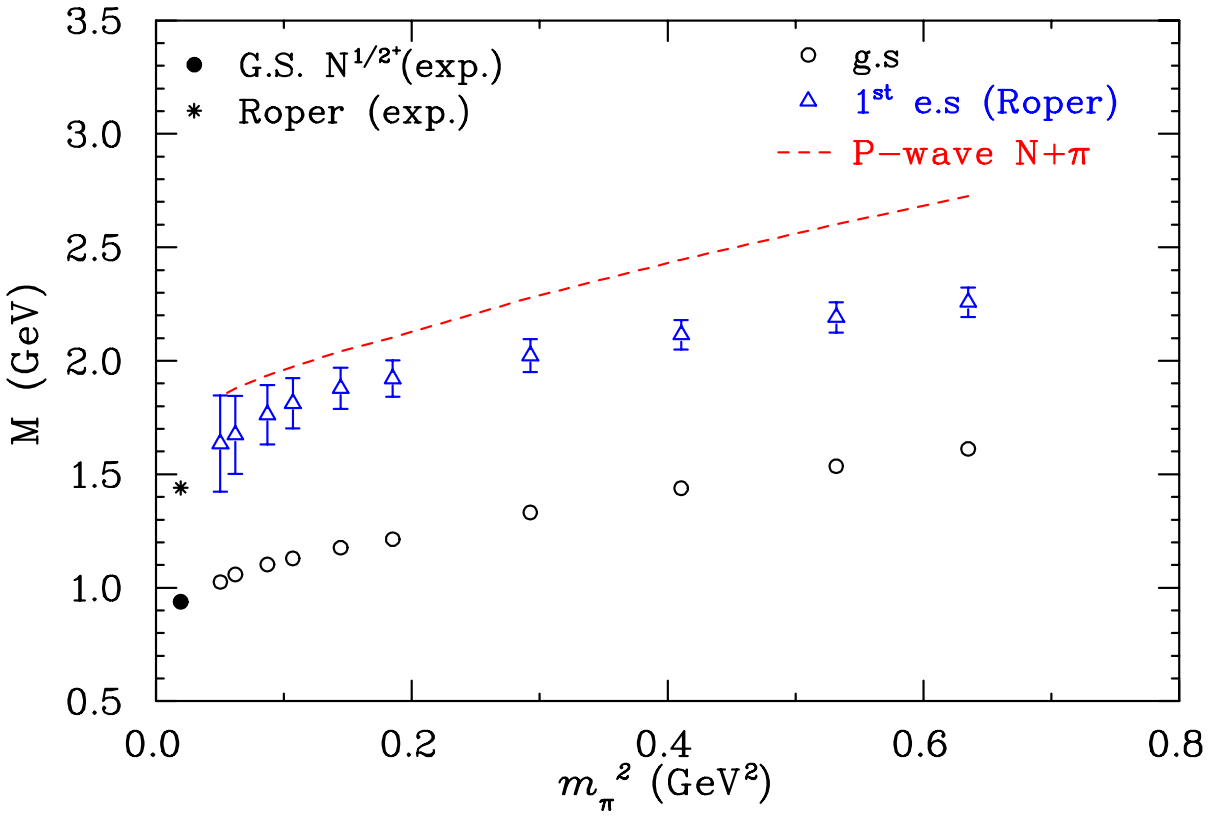

Figure 4: (Color online). The ground and the Roper states and the non-interacting P-wave $N + \pi$ are illustrated. The black filled symbols are the experimental values of the ground and the Roper states obtained from Ref. [47].

Euclidean-time from the heaviest to the lightest quarks masses.

There are quenched artifacts that will have significant influence on our results should we progress to lighter quark masses. Not only are πN couplings different in quenched QCD, but there are also contributions from unphysical, degenerate P-wave $\eta' N$ two-particle states [14]. Future calculations approaching the decay threshold should be done in full dynamical-fermion QCD.

In conclusion, through the use of a variety of smeared-smeared correlation functions in constructing the correlation matrix, the first positive parity excited state of the nucleon $N^{\frac{1}{2}^+}$, the Roper state, has been observed for the first time using the variational analysis. While the 3×3 correlation matrix analysis of standard interpolators is insufficient to isolate these excited energy eigenstates of QCD [16], using the new correlation matrix construction with smeared-smeared correlators enables us to extract the otherwise elusive Roper state.

Acknowledgments

We thank the NCI National Facility and eResearch SA for generous grants of supercomputing time which have enabled this project. This research is supported by the Australian Research Council.

References

[1] N. Isgur, G. Karl, Phys. Lett. B72 (1977) 109.
[2] N. Isgur, G. Karl, Phys. Rev. D19 (1979) 2653.
[3] Z.-p. Li,V. Burkert, Z.-j. Li, Phys. Rev. D46 (1992) 70–74.
[4] C. E. Carlson, N. C. Mukhopadhyay, Phys. Rev. Lett. 67 (1991) 3745–3748.
[5] P. A. M. Guichon, Phys. Lett. B164 (1985) 361.
[6] O. Krehl,C. Hanhart,S. Krewald, J. Speth, Phys. Rev. C62 (2000) 025207. arXiv:nucl-th/9911080,
[7] D. B. Leinweber, Phys. Rev. D51 (1995) 6383–6393. arXiv:nucl-th/9406001.
[8] F. X. Lee, D. B. Leinweber, Nucl. Phys. Proc. Suppl. 73 (1999) 258–260. arXiv:hep-lat/9809095,
[9] M. Gockeler, et al., Phys. Lett. B532 (2002) 63–70. arXiv:hep-lat/0106022,
[10] S. Sasaki,T. Blum, S. Ohta, Phys. Rev. D65 (2002) 074503. arXiv:hep-lat/0102010.
[11] W. Melnitchouk, et al., Phys. Rev. D67 (2003) 114506. arXiv:hep-lat/0202022.
[12] R. G. Edwards,U. M. Heller, D. G. Richards, Nucl. Phys. Proc. Suppl. 119 (2003) 305–307. arXiv:hep-lat/0303004,
[13] F. X. Lee, et al., Nucl. Phys. Proc. Suppl. 119 (2003) 296–298. arXiv:hep-lat/0208070.
[14] N. Mathur, et al., Phys. Lett. B605 (2005) 137–143. arXiv:hep-ph/0306199.
[15] S. Sasaki, Prog. Theor. Phys. Suppl. 151 (2003) 143–148. arXiv:nucl-th/0305014.
[16] M. S. Mahbub, et al. arXiv:0905.3616.
[17] D. Guadagnoli,M. Papinutto, S. Simula, Phys. Lett. B604 (2004) 74–81. arXiv:hep-lat/0409011.
[18] K. Sasaki,S. Sasaki, T. Hatsuda, Phys. Lett. B623 (2005) 208–217. arXiv:hep-lat/0504020.
[19] C. Michael, Nucl. Phys. B259 (1985) 58.
[20] M. Luscher, U. Wolff, Nucl. Phys. B339 (1990) 222–252.
[21] C. McNeile, C. Michael, Phys. Rev. D63 (2001) 114503. arXiv:hep-lat/0010019.
[22] B. Blossier,M. Della Morte,G. von Hippel,T. Mendes, R. Sommer, JHEP 04 (2009) 094. arXiv:0902.1265,
[23] C. R. Allton, et al., Phys. Rev. D47 (1993) 5128–5137. arXiv:hep-lat/9303009.
[24] J. N. Hedditch,D. B. Leinweber,A. G. Williams, J. M. Zanotti, Nucl. Phys. Proc. Suppl. 128 (2004) 221–226. arXiv:hep-lat/0402016.
[25] B. G. Lasscock, et al., Phys. Rev. D76 (2007) 054510. arXiv:0705.0861,
[26] D. Brommel, et al., Phys. Rev. D69 (2004) 094513. arXiv:hep-ph/0307073.
[27] T. Burch, et al., Phys. Rev. D70 (2004) 054502. arXiv:hep-lat/0405006.
[28] T. Burch, et al., Nucl. Phys. Proc. Suppl. 140 (2005) 284–286. arXiv:hep-lat/0409014,
[29] T. Burch, et al., Nucl. Phys. A755 (2005) 481–484. arXiv:nucl-th/0501025,
[30] B. G. Lasscock, et al., Phys. Rev. D72 (2005) 014502. arXiv:hep-lat/0503008.
[31] T. Burch,C. Gattringer,L. Y. Glozman,C. Hagen, C. B. Lang, Phys. Rev. D73 (2006) 017502. arXiv:hep-lat/0511054,
[32] T. Burch, et al., Phys. Rev. D73 (2006) 094505. arXiv:hep-lat/0601026.
[33] T. Burch, et al., Phys. Rev. D74 (2006) 014504. arXiv:hep-lat/0604019.
[34] T. Burch, et al., PoS LAT2005 (2006) 075. arXiv:hep-lat/0509051.
[35] T. Burch, et al., PoS LAT2005 (2006) 097. arXiv:hep-lat/0509086.
[36] S. Basak, et al., Nucl. Phys. Proc. Suppl. 153 (2006) 242–249. arXiv:hep-lat/0601034,
[37] S. Basak, et al., Phys. Rev. D76 (2007) 074504. arXiv:arXiv:0709.0008[hep-lat].
[38] S. Gusken, Nucl. Phys. Proc. Suppl. 17 (1990) 361–364.
[39] T. Takaishi, Phys. Rev. D54 (1996) 1050–1053.
[40] P. de Forcrand, et al., Nucl. Phys. B577 (2000) 263–278. arXiv:hep-lat/9911033,
[41] J. M. Zanotti, et al., Phys. Rev. D65 (2002) 074507. arXiv:hep-lat/0110216.
[42] J. M. Zanotti,B. Lasscock,D. B. Leinweber, A. G. Williams, Phys. Rev. D71 (2005) 034510. arXiv:hep-lat/0405015.
[43] R. Sommer, Nucl. Phys. B411 (1994) 839–854. arXiv:hep-lat/9310022,
[44] C. Morningstar, M. J. Peardon, Phys. Rev. D69 (2004) 054501. arXiv:hep-lat/0311018,
[45] B. G. Lasscock, et al., Phys. Rev. D72 (2005) 074507. arXiv:hep-lat/0504015.
[46] D. B. Leinweber,R. M. Woloshyn, T. Draper, Phys. Rev. D43 (1991) 1659–1678.
[47] W. M. Yao, et al., J. Phys. G33 (2006) 1–1232.